

# Precision of morphogen-driven tissue patterning during development is enhanced through contact-mediated cellular interactions

Chandrashekar Kuyyamudi,<sup>1,2</sup> Shakti N. Menon,<sup>1</sup> and Sitabhra Sinha<sup>1,2</sup>

<sup>1</sup>*The Institute of Mathematical Sciences, CIT Campus, Taramani, Chennai 600113, India*

<sup>2</sup>*Homi Bhabha National Institute, Anushaktinagar, Mumbai 400 094, India*

(Dated: October 26, 2021)

Embryonic development involves pattern formation characterized by the emergence of spatially localized domains characterized by distinct cell fates resulting from differential gene expression. The boundaries demarcating these domains are precise and consistent within a species despite stochastic fluctuations in the morphogen molecular concentration that provides positional information to the cells, as well as, the intrinsic noise in molecular processes that interpret this information to guide fate determination. We show that local interactions between physically adjacent cells mediated by receptor-ligand binding utilizes the asymmetry between the fate-determining genes to yield a switch-like response to the global signal provided by the morphogen. This results in robust developmental outcomes with a consistent identity of the gene that is dominantly expressed at each cellular location, thereby substantially reducing the uncertainty in the location of the boundary between distinct fates.

The ubiquity of noise in the natural world makes it imperative that biological processes are robust to it [1, 2]. This is particularly relevant during the development of an organism as small deviations resulting from chance events at earlier stages can get amplified over time leading to pathological outcomes [3, 4]. Indeed, embryos exhibit a highly reproducible sequence of cellular division, differentiation and rearrangement resulting in a physiological organization that is consistent across all individuals of a species [5–7]. Morphogenesis involves pattern formation [8, 9] in which cells at various locations in a tissue adopt distinct specialized roles (fates) via differential gene expression. This is often guided by concentration gradients of molecules known as morphogens that emerge via diffusion from localized sources [Fig. 1 (a)]. Each cell responds to the local morphogen concentration in its immediate neighborhood and attains a fate determined by whether the concentration lies between a specific pair of thresholds [10–13]. The resulting domains with different fates are characterized by sharp boundaries whose locations are invariant for a species, e.g., that occurring between cells expressing dorsal and ventral fates in an embryo [shown in Fig. 1 (b) for *Xenopus*]. This is surprising as, in order to adopt a fate consistent with its position, a cell must correctly infer its location in the tissue from the information provided by the morphogen concentration signal, which is very noisy due to fluctuations in the synthesis, degradation and diffusive transport of molecules [Fig. 1 (a), inset] [12, 14–16]. In addition, each of the steps involved in the intra-cellular response, from binding of morphogen with surface receptors to the downstream signaling cascade terminating in gene expression, is inherently noisy because of the underlying probabilistic processes involving a small number of molecules involved ( $\ll N_o$ , Avogadro’s number) [17–19].

Fig. 1 (c) shows that, in the absence of any explicit mechanism for noise reduction, the expression levels of a pair of patterning genes *A* and *B* in the cells of a model system responding to the local morphogen con-

centration are subject to a high degree of variation. The expression levels are observed to be comparable over a number of cells such that neither gene is guaranteed to dominate and hence determine the fate, suggesting that the cell fates are primarily decided by random chance events [20, 21]. This would result in the length of the domains comprising cells with different fates varying considerably across realizations, which contrasts sharply with the highly reproducible spatial pattern that is expected [Fig. 1 (d)]. Thus, processes that aid in reducing variability must underlie the high level of precision in fate boundaries observed during development [22, 23]. Among the several candidate mechanisms that have been proposed, many involve making the behavior of the morphogen interpretation module within each cell more robust, e.g., incorporating the dynamics of genetic regulatory networks [23–26]. Alternatively, consistency in cell fate decision-making can be promoted by regulating the nature of the morphogen concentration gradient so as to reduce fluctuations in it [21, 27, 28]. In general, all such mechanisms that improve the reliability of cellular decision-making based on their spatial location can be considered to effectively pool together information gathered from multiple measurements of the morphogen signal in the immediate neighborhood [6]. While for a single cell, this typically involves temporal integration of the signal, the same aim can potentially be achieved by neighboring cells sharing information about the morphogen concentration that they each detect [29]. As in the developing embryo, cells in close physical proximity are known to communicate with each other through contact-mediated signaling, such inter-cellular interactions can be a possible mechanism through which spatial integration of the morphogen signal can be implemented [6, 30]. One of the most widely observed examples of such interactions is the evolutionarily conserved Notch signaling pathway [31–34], which is triggered by Notch receptors on the surface of a cell binding to membrane-bound proteins (e.g., Delta ligand) of

a neighboring cell. Indeed, Notch-mediated interactions are known to have a fundamental role in all metazoan development [31, 35]. Although it has been suggested earlier that such contact-mediated signaling may play a role in regulating noise [6, 36, 37], the mechanism through which this can arise is yet to be established.

In this paper we have demonstrated that the precision of the boundary between domains expressing different cell fates is improved considerably when cells can communicate via Notch signaling. Specifically, we investigate the role played by such signals in regulating the expression of mutually inhibiting patterning genes ( $A$ ,  $B$ ) that determine the developmental fate of a cell. Noise, in the form of stochastic fluctuations in the concentration of the morphogen, as well as, in that of the signaling molecules and the expression levels of the patterning genes, results in a high degree of variability in the fate adopted by each cell in isolation. However, when the downstream effector ( $S$ ) of the Notch signaling pathway is allowed to upregulate the patterning gene that can express at a lower morphogen concentration (assumed to be  $A$ ) compared to the other, we observe a remarkable decrease in the uncertainty in the fate of a cell at a particular location in the tissue. The effectively equivalent interaction in which the other gene ( $B$ ) is downregulated by the signal also shows a qualitatively similar outcome. In contrast, for interactions of the opposite type (viz.,  $S$  upregulating  $B$  or downregulating  $A$ ), an increase in the sharpness of fate boundaries is seen over a more limited region of the relevant parameter space. Insight into the process by which the coupling counters noise is provided by the observation that robustness requires the time-scale of the contact-induced signal to be longer than those associated with gene expression dynamics. Our results show that Notch signaling between cells is capable of exploiting any inherent asymmetry in the interactions between patterning genes and their response to the morphogen, yielding a highly robust developmental outcome.

To investigate the potential role of contact-mediated interaction between cells in generating robust spatial patterns from position-dependent cell fate determination in the presence of stochastic fluctuations, we consider a linear array of cells that are subject to a morphogen concentration gradient. The source from which the morphogen molecules are secreted at a constant rate  $\alpha_M$  is assumed to be located at one end of the array. The molecules, that decay after a mean lifetime  $\tau_M$ , randomly disperse in a medium having diffusion coefficient  $D_M$  across the array, resulting in their concentration exhibiting fluctuations around an exponentially decaying spatial profile. The temporally averaged signal strength sensed by a cell located at a distance  $x$  away from the source is  $M(x) = M(0) \exp(-x/\lambda_M)$ , where  $\lambda_M$  is the characteristic length scale associated with the gradient. At any instant, the magnitude of the signal governs the expression of genes comprising the morphogen interpretation module. We choose the simplest non-trivial example of differential gene expression leading to spatial patterning,

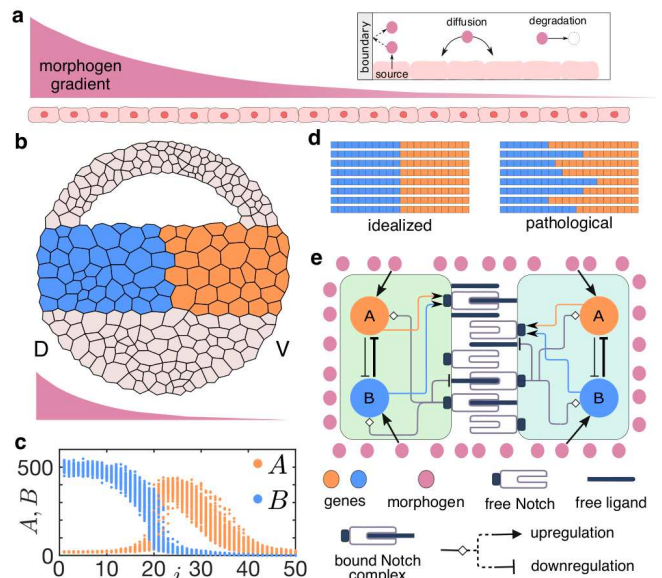


**FIG. 1. Cell fate determination through a morphogen concentration gradient needs to be robust against stochastic fluctuations.** (a) A morphogen gradient across a cellular array results from the processes (shown in the inset) of secretion of molecules from a source located at the boundary of the domain, their diffusion across space and degradation over time such that the decay rate is linearly proportional to its concentration. (b) Schematic representation of a *Xenopus* embryo where the differentiation of the cells of the mesoderm into dorsal and ventral fates (represented by blue and orange, respectively) is guided by the concentration gradient of the morphogen *activin* between the dorsal (D) and ventral (V) ends (displayed below the embryo). (c) The steady state expression of patterning genes  $A$ ,  $B$  across a 1-dimensional array comprising  $N$  cells, with the indices of the cells indicated by  $i = 1, \dots, N (= 50)$ , subject to a noisy morphogen gradient in the absence of interaction between the cells. Results of 300 different realizations are shown. (d) While in the absence of noise the boundary separating the regions with the two different fates corresponding to  $B > A$  (blue) and  $A > B$  (orange) is expected to occur at the same position across all realizations (the idealized situation shown at left), fluctuations in the morphogen concentration and gene expression dynamics results in variations across realizations (shown at right) if fate determination occurs only on the basis of positional information provided by the morphogen gradient. (e) Interactions between neighboring cells mediated by Notch-Delta signaling pathway (shown here schematically) can aid in the robust determination of fate boundaries in the presence of noise. Genes  $A$  and  $B$  comprising the morphogen interpretation module affect the expression of genes coding for Notch receptors. The Notch Intracellular Domain (NICD), released from the bound Notch complex that results from the *trans*-activation of Notch receptors, in turn up- or downregulates the expression of  $A$  and  $B$  (depending on the type of interaction).

viz., a module having two genes,  $A$  and  $B$  [Fig. 1 (e)]. As is characteristic of gene circuits that respond to the concentration of an external morphogen, the two patterning genes are assumed to mutually repress each other, fa-

voring the dominance of one over the other in terms of expression levels [12, 38]. The maximally expressed gene among the two within each cell decides its corresponding fate. For example, in the context of mesoderm differentiation in *Xenopus* in the presence of the morphogen *activin*, they can be identified with the genes *Goosecoid* and *Brachyury* [39, 40]. Here we focus on the location of the fate boundary that demarcates regions with high levels of expression of *A* from those of *B*.

As mentioned above, the expression of gene *A* occurs at relatively low values of the signal, unlike gene *B* which needs higher concentration of the morphogen. Thus, to prevent a homogeneous fate for the entire domain, we need to ensure that higher concentrations of the morphogen favor the expression of *B*. This is achieved by an asymmetric mutual repression such that *B* inhibits *A* more strongly than *A* does *B*. Contact-mediated interaction between cells is implemented by coupling the patterning gene expression dynamics of adjacent cells through Notch signaling [31, 35]. Specifically, when both genes are expressed at high levels in a cell, it results in upregulation of the gene encoding Notch, leading to an increased concentration of free receptors (*R*). This enhances the strength of contact-mediated interactions by increasing the the probability of a binding event. The trans-activation of Notch receptors upon binding to a Delta ligand of a neighboring cell leads to a downstream effector *S* of the resulting signaling cascade regulating the expression of the patterning genes. Based on whether *S* up or downregulates the expression of gene *A* or gene *B*, we can classify the intercellular interactions into four different types. We report below in detail the dynamical consequences of each type of coupling. The signaling resulting from trans-activation of Notch receptors also results in the repression of the production of Delta ligand protein [32, 41], thereby decreasing the concentration of free ligands (*D*).

The equations describing the stochastic dynamics of all variables  $\mathbf{X} : \{M, A, B, R, D, S\}$  in our model have the form  $d\mathbf{X} = \mathcal{F}_\mathbf{X} dt + \mathcal{G}_\mathbf{X} dW$ , with the stochastic component being  $\mathcal{G}_\mathbf{X} = \eta \mathbf{X}$  where  $\eta$  is the strength of the noise and  $dW$  is a Wiener process [42, 43], while the deterministic component  $\mathcal{F}$  for the different variables of the system are given by:

$$\begin{aligned} \mathcal{F}_M &= \alpha_M \delta_{i,1} - D_M \nabla^2 M - \frac{M}{\tau_M}, \\ \mathcal{F}_A &= \alpha_A \mathcal{H}_h(M, K_1) \mathcal{H}'_h(B, K_3) \Phi_A + \gamma_A \mathcal{H}_g(S, Q) - \frac{A}{\tau_A}, \\ \mathcal{F}_B &= \alpha_B \mathcal{H}_h(M, K_2) \mathcal{H}'_h(A, K_4) \Phi_B + \gamma_B \mathcal{H}_g(S, Q) - \frac{B}{\tau_B}, \\ \mathcal{F}_R &= \beta_{R_0} + \beta_R \mathcal{H}_g(A, J) \mathcal{H}_g(B, J) - k_{tr} R D_{tr} - \frac{R}{\tau_R}, \\ \mathcal{F}_D &= \beta_{D_0} + \beta_D \mathcal{H}'_g(S, K_5) - k_{tr} R D_{tr} - \frac{D}{\tau_D}, \\ \mathcal{F}_S &= k_{tr} R D_{tr} - \frac{S}{\tau_S}, \end{aligned}$$

where  $R_{tr}$  and  $D_{tr}$  refers to the total concentrations of receptors and ligands, respectively, in the neighboring cell(s). The Hill functions corresponding to activation and inactivation of *X* are described as  $\mathcal{H}_\beta(X, C) = X^\beta / (C^\beta + X^\beta)$  and  $\mathcal{H}'_\beta(X, C) = C^\beta / (C^\beta + X^\beta)$ , respectively, with  $C$  as the half-saturation constant and  $\beta$  being the Hill exponent. The functions  $\Phi_A, \Phi_B$  and parameters  $\gamma_A, \gamma_B$  characterize the four distinct types of inter-cellular interactions and are defined in Table I.

	$\Phi_A$	$\Phi_B$	$\gamma_A$	$\gamma_B$
$S \dashv B$	1	$Q^g / Q^g + S^g$	0	0
$S \rightarrow A$	1	1	$>0$	0
$S \dashv A$	$Q^g / Q^g + S^g$	1	0	0
$S \rightarrow B$	1	1	0	$>0$

TABLE I. Description of the functions and parameters defining the four different types of inter-cellular signaling considered, based upon the nature of interaction, viz., upregulation ( $\rightarrow$ ) or downregulation ( $\dashv$ ), and the identity of the patterning gene whose expression is regulated by the Notch downstream effector *S*, i.e., *A* or *B*.

To quantitatively characterize the role of inter-cellular interaction in promoting robustness to noise, we compare the variance of the spatial location of the fate boundary when the cells interact via Notch signaling, with the case when the cells attain their fates independent of their neighbors. The situation when the cells are uncoupled is shown in Fig 1 (c), which displays the spatial distribution of steady state expression values of the patterning genes. It is seen that in cells close to the fate boundary (i.e.,  $i \sim 20$ ) the level of expression of both genes vary over a large range, with a substantial degree of overlap between the two distributions. As a result, the fates attained by each of these cells vary from one realization to another [Fig 1 (d), right], which suggests that they have insufficient positional information for their eventual identities to be determined with any certainty. This ambiguity in cell fates can lead to a biologically undesirable outcome, viz., high variability in embryonic patterning across individuals of a species.

The strength of the interaction between Notch signaling and patterning gene expression dynamics is regulated in our model by the parameters  $Q, J$  and  $K_5$  (see the expressions for  $\mathcal{F}_{A,B}, \mathcal{F}_R$  and  $\mathcal{F}_D$ , respectively, defined above). Two additional parameters  $\gamma_A$  and  $\gamma_B$  also play a role but only when the signal *S* upregulates the patterning genes (see Table I). Here we focus on the two half-saturation constants  $Q$  and  $J$ , where  $Q$  is the magnitude of *S* above which the signal noticeably affects patterning gene expression, while  $J$  determines the expression levels of the patterning genes above which production of Notch receptors is appreciably increased. The parameter  $K_5$  which controls the strength of repression of the Delta ligand by the Notch signal also contributes to the final outcome. However, as the coupling-induced suppression of noise occurs even when *S* has no effect on

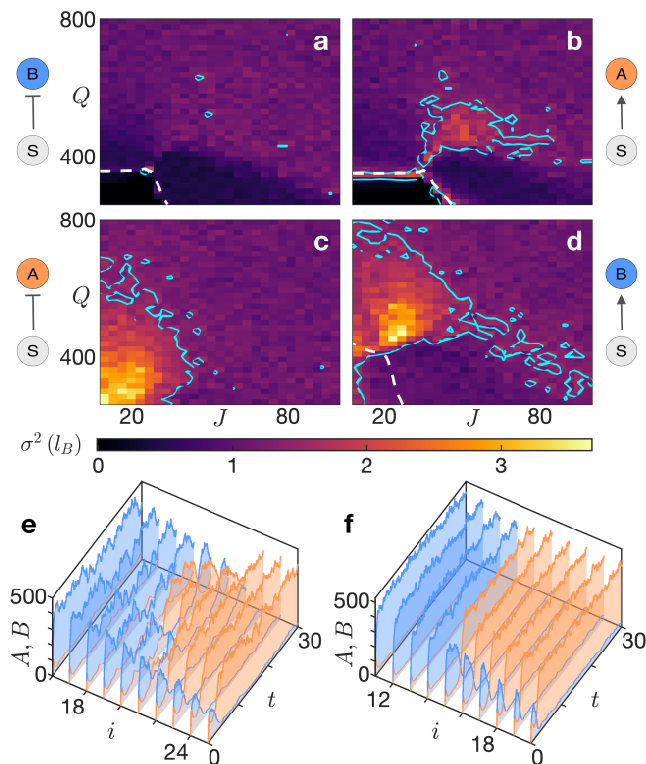


**FIG. 2. Robust determination of cell fates results from interaction between stochastic gene expression dynamics and contact-mediated signaling.** The intercellular interactions mediated by the Notch downstream signal ( $S$ ) can be classified into four types, determined by which of the patterning genes ( $A$  or  $B$ ) is either up or downregulated by  $S$ , as represented by the motifs shown beside each panel (a-d) [arrows representing up/downregulation are as indicated in Fig. 1 (e)]. For each type, the spatial pattern formed by cells adopting distinct fates  $A$ ,  $B$  in a 1D domain comprising  $N (= 50)$  cells subject to a morphogen gradient is characterized by the location  $l_B$  of the boundary [ $\sim 20$ , in absence of any interactions between the cells, see Fig. 1 (c)] demarcating the segments expressing the two fates. The variance in  $l_B$  across 300 stochastic realizations is shown for each choice of the pair of parameters quantifying the strength of intercellular coupling, viz.,  $J$  representing critical value of patterning gene expression segregating low/high receptor production and  $Q$  representing critical signal intensity that distinguishes between weak and strong regulation of patterning gene expression. The continuous curves in each panel are contours indicating the variance in  $l_B$  in the absence of intercellular interactions ( $\simeq 1.38$ ). The regions in the  $J - Q$  plane above the broken curves (shown in white) correspond to the mean value of  $l_B$  lying within  $[10, 30]$ , i.e., 50% of its value in the uncoupled case. Note that, for coupling types in which  $S$  upregulates  $A$  either directly (b), or indirectly via suppression of its inhibitor  $B$  (a), fluctuations in  $l_B$  are markedly reduced over a wider range of  $J$  and  $Q$ . (e-f) Temporal evolution of the expression of  $A$  and  $B$  shown for cells around  $l_B$  for the uncoupled case, contrasting (e) the dynamics seen in absence of any intercellular interactions, with (f) that obtained when  $S$  inhibits  $B$  [as in panel (a)]. While the uncoupled cells exhibit large fluctuations in expression levels with uncertainty in  $l_B$  sustained for a long time, in the presence of intercellular interactions cells rapidly converge to their eventual fates.

$D$  production, we may conclude that the phenomenon is not critically dependent on the value of  $K_5$ .

Fig. 2 shows the dispersion in the fate boundary position in a linear array of  $N$  cells coupled via Notch-Delta signaling as each of the parameters  $Q$  and  $J$  are varied over a large range, for the four distinct types of intercellular interactions mentioned above. While for all interactions we observe regions exhibiting a substantial reduction in the extent to which the location  $l_B$  of the fate boundary fluctuates across realizations, this is most prominent when the interaction involves either  $S$  downregulating the expression of  $B$  [Fig. 2 (a)], or equivalently, upregulating the expression of its inhibitor  $A$  [Fig. 2 (b)]. We observe not only a much larger area of the  $Q - J$  parameter space where the variance  $\sigma^2(l_B)$  is lower than that for the case when inter-cellular interactions are absent, but also a relatively greater certainty with which the domains exhibiting different fates are demarcated for these two types of interactions.

This enhanced robustness of the cell fate pattern when  $S$  suppresses  $B$  (or equivalently, promotes  $A$ ) can be understood in terms of the alteration in the steady-state level of expression of the patterning genes around the fate boundary. In the absence of coupling, not only are the expression levels of both genes distributed over a larger range for each cell, but the two distributions also exhibit a substantial degree of overlap [Fig. 3 (a)]. This suggests that the identity of the gene which eventually dominates at the steady state (and hence decides the fate) for any cell close to the boundary is largely decided by stochastic perturbations. In contrast, the inter-cellular interactions result in suppression of the patterning gene  $B$  by  $S$  specifically in the region of the array where the two patterning genes are expressed at comparably high levels ( $> J$ ) and consequently, where the two distributions overlap. Thus, we observe from Fig. 3 (b) that for cells ( $i \geq 13$ ) where both  $A, B > J$  in the steady state for the uncoupled case, the Notch-mediated interaction leads to the dominance of  $A$  over  $B$  consistently across all realizations. The repression of  $B$  by  $A$  results in the peaks of their respective distributions becoming widely separated. For cells closer to the morphogen source ( $i \leq 12$ ),  $B$  dominates because of the asymmetric strength of mutual repression between the two patterning genes mentioned earlier, resulting in low expression levels of  $A$  and consequently, negligible production of  $S$ . Hence, for these cells also we observe widely separated peaks for  $A$  and  $B$  distributions, but with the latter occurring at higher values (as in the uncoupled case). The inter-cellular interactions can, thus, be seen as enhancing the distinction between the steady-state levels of  $A$  and  $B$ , the elimination of overlap between the two distributions leading to a sharply defined fate boundary [Fig. 3 (c), compare with Fig. 1 (c)]. Note that boundary shifts closer to the morphogen source (with respect to its location in the uncoupled case), as the inter-cellular interactions in which  $S$  suppresses  $B$  (or promotes  $A$ ) favors the dominance of  $A$  where the two overlap in the absence of interactions. Our model,

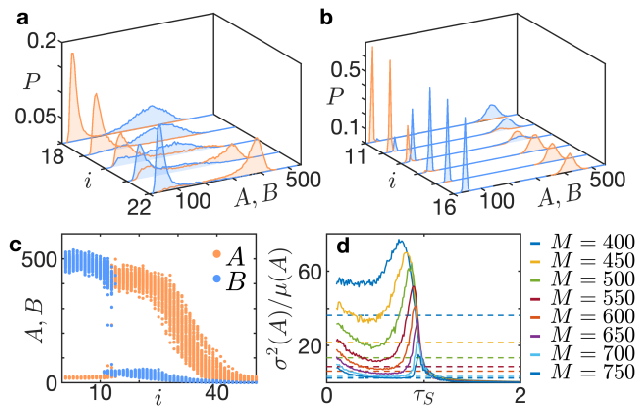


**FIG. 3. Reduction in variability of response to fluctuating morphogen concentrations depends on relative time-scales of gene expression dynamics and contact-mediated signaling.** (a-b) Steady-state distributions for the expression levels of the patterning genes  $A$  and  $B$  shown for cells located around the respective positions of the fate boundary when (a) intercellular interactions are absent, or (b) the Notch downstream signal  $S$  suppresses expression of  $B$  [as in Fig. 2 (a)]. In the uncoupled case, the distributions are extremely broad with a high degree of overlap close to the fate boundary, indicating a large degree of uncertainty in the identity of the gene having higher expression levels, and hence in the fate of the corresponding cells. Intercellular interactions result in the gene expressions exhibiting sharply defined peaks at either very low or very high levels, with the gene that is dominantly expressed at any given cell clearly identifiable. This leads to a steady state expression of the patterning genes [shown in (c) for a 1-dimensional array comprising 50 cells] that exhibits a robust, sharply defined cell fate boundary (at  $i \approx 12$ ) even in the presence of a noisy morphogen gradient. Results of 300 different realizations are shown. (d) Temporal variance in the expression of gene  $A$  in a given cell, expressed relative to its mean value, shown as a function of the mean lifetime  $\tau_S$  of the Notch downstream signal  $S$ . For different mean concentrations  $M$  (indicated by distinct colors, see legend) of the morphogen, a peak is observed at a critical value of  $\tau_S$  above which the system is effectively insensitive to fluctuations. For each  $M$ , a broken horizontal line (of the same color) represents the corresponding variance:mean ratio for the uncoupled case, i.e., in the absence of the Notch signal.

thus, helps explain the shift in fate boundary that has been observed when cells communicate via Notch signaling [44, 45]. Consistent with this explanation, the reverse is observed for types of interaction where  $S$  instead suppresses  $A$  (or promotes  $B$ ) with the fate boundary location moving further away from the morphogen source [see Supplementary Information].

The mechanism of interaction between  $S$  and the patterning genes can be made more transparent by considering a simplified scenario where the *trans* ligand concentration in the neighborhood that stimulates the receptors of a cell is assumed to be time-invariant. Such an approximation is still capable of reproducing the phenomenon of noise-suppression, which is not crucially dependent on the dynamics of  $D$ . We investigate the patterning gene

expression dynamics in the cells of such a system, subjected to stochastic fluctuations in morphogen concentration (around the mean value  $M$ ) and intrinsic noise. Fig. 3 (d) shows the relative variance in the expression of gene  $A$  ( $B$  exhibits qualitatively similar behavior, see Supplementary Information) as a function of the mean lifetime  $\tau_S$  of the downstream effector for the Notch signaling pathway. We observe that independent of the mean morphogen concentration (and hence, the position of a cell on an array that is subject to a morphogen gradient), the gene expression level becomes extremely robust to noise when  $\tau_S$  is sufficiently large ( $\gtrsim 1$ ). To understand this, we note from the expression for  $\mathcal{F}_S$  (see equation above) that increasing  $\tau_S$  results in a proportionately higher steady state value of  $S$  that a cell is subjected to. Focusing on the interaction in which  $S$  downregulates  $B$  expression, we note that for high values of  $S$  the dynamics of  $B$  is altered as the function  $\Phi_B$  essentially reduces to zero (for reasonably high values of the Hill exponent  $g$ ). The resultant sharp decrease in the production terms in  $\mathcal{F}_B$  implies that  $A$  will dominate  $B$  in all cells where  $S$  is high. As the magnitude of the signal also depends on receptor concentration, whose production is high only for those cells in which both  $A$  and  $B$  are expressed at sufficiently high levels ( $> J$ ), the  $S$ -induced suppression of  $B$  will only be observed in those cells where the distributions of the patterning genes overlap considerably. Similar behavior will be seen for the interaction where  $S$  upregulates expression of  $A$ , as the latter inhibits  $B$  leading to effective downregulation of  $B$  by  $S$ .

For the type of interaction in which the signal downregulates  $A$  (or equivalently, upregulates  $B$ ), the function  $\Phi_A$ , and hence the production term in  $\mathcal{F}_A$ , decreases to very low values for large  $S$ . As a result,  $B$  is favored to dominate over  $A$  in the region where the patterning genes are expressed at comparable levels when the cells are uncoupled. This would lead one to expect an analogous situation to that described above but with  $B$  replacing  $A$  as the preferred cell fate around the fate boundary location for the non-interacting case. However, as this region is located relatively far from the morphogen source, the local concentration of  $M$  may not be high enough to promote the expression of  $B$  while being sufficient for the expression of  $A$  (as  $K_2 > K_1$ ). As a result, the advantage conferred to  $B$  by the contact-mediated interaction is offset by the low morphogen concentration that favors  $A$ , preventing outright dominance by either gene in this region. Hence, these two types of interactions between  $S$  and the patterning genes are unable to reduce the variability in fate boundary position for a wide range of choices of the parameters  $Q$  and  $P$  [Fig. 2 (c-d)].

To conclude, we have shown that contact-mediated interaction between cells (e.g., via downstream signaling triggered by binding of Notch receptors on a cell surface with the surface-bound ligands of its neighbors) can reduce the uncertainty in cell fates that arise from stochastic fluctuations in the morphogen concentration that provides positional information to the cells, as well as, in-

trinsic noise. Even though the signaling mechanism we employ is also subject to random variability in its components, the coupling between cells that it effects is able to markedly reduce the dispersion in the position of the boundary between regions expressing distinct cell fates and thus enhancing robustness of spatial patterns arising in tissues and organs over the course of development. Our results suggest a functional role for the higher level of Notch signaling observed in the cells demarcating the boundary between the regions expressing dorsal and ventral fates in the *Drosophila* hindgut [46]. Notch activity is also known to be crucial for defining the boundaries of the organ of corti in the cochlea of mice, consistent with the mechanism outlined here [47]. A more direct experimental test of our model can involve verifying that those regions in tissue undergoing differentiation, whose cells have comparable levels of expression for the different patterning genes, exhibit higher levels of Notch activity. The results reported here show that the nature of interaction between the downstream effector of the intercellular signaling mechanism and the patterning gene(s) is

important in determining the extent to which coupling between cells enhance the robustness of cell fate patterns. In particular, they suggest that the mechanism is more effective in suppressing noise and reducing variability when Notch signaling upregulates that patterning gene (or equivalently, downregulates the gene repressing it) which requires a relatively lower concentration of the morphogen to be expressed. This is a potential experimental test for the proposed model, involving comparison of expression levels of different patterning genes in the presence of inter-cellular interactions with that observed in its absence (e.g., implemented by knocking out Notch).

We would like to thank Marcin Zagórski for helpful discussions. SNM has been supported by the IMSc Complex Systems Project (12th Plan), and the Center of Excellence in Complex Systems and Data Science, both funded by the Department of Atomic Energy, Government of India. The simulations required for this work were supported by IMSc High Performance Computing facility (hpc.imsc.res.in) [Nandadevi].

- 
- [1] H. Kitano, *Nat. Rev. Genet.* **5**, 826 (2004).  
 [2] L. S. Tsimring, *Rep. Prog. Phys.* **77**, 026601 (2014).  
 [3] C. H. Waddington, *The Strategy of the Genes* (George Allen & Unwin, London, 1957).  
 [4] L. Wolpert, C. Tickle, and A. M. Arias, *Principles of Development* (Oxford University Press, USA, 2015).  
 [5] P. W. Sternberg, *Science* **303**, 637 (2004).  
 [6] A. D. Lander, *Science* **339**, 923 (2013).  
 [7] S. Gilbert, *Developmental Biology* (Sinauer, Sunderland, MA, 2013).  
 [8] M. C. Cross and P. C. Hohenberg, *Rev. Mod. Phys.* **65**, 851 (1993).  
 [9] A. J. Koch and H. Meinhardt, *Rev. Mod. Phys.* **66**, 1481 (1994).  
 [10] L. Wolpert, *J. Theor. Biol.* **25**, 1 (1969).  
 [11] L. Wolpert, *Development* **107**, 3 (1989).  
 [12] J. B. Gurdon and P.-Y. Bourillot, *Nature* **413**, 797 (2001).  
 [13] J. Sharpe, *Development* **146**, dev185967 (2019).  
 [14] A. D. Lander, Q. Nie, and F. Y. Wan, *Dev. Cell* **2**, 785 (2002).  
 [15] G. Hornung, B. Berkowitz, and N. Barkai, *Phys. Rev. E* **72**, 041916 (2005).  
 [16] A. Kicheva, P. Pantazis, T. Bollenbach, Y. Kalaidzidis, T. Bittig, F. Jülicher, and M. González-Gaitán, *Science* **315**, 521 (2007).  
 [17] M. B. Elowitz, A. J. Levine, E. D. Siggia, and P. S. Swain, *Science* **297**, 1183 (2002).  
 [18] M. Kærn, T. C. Elston, W. J. Blake, and J. J. Collins, *Nat. Rev. Genet.* **6**, 451 (2005).  
 [19] A. M. Arias and P. Hayward, *Nat. Rev. Genet.* **7**, 34 (2006).  
 [20] X.-D. Zheng, J. Mei, D.-H. Chen, and Y. Tao, *Phys. Rev. E* **98**, 042406 (2018).  
 [21] A. Guillemin and M. P. H. Stumpf, *Phys. Biol.* **18**, 011002 (2020).  
 [22] M. M. K. Hansen, W. Y. Wen, E. Ingerman, B. S. Ra-zoosky, C. E. Thompson, R. D. Dar, C. W. Chin, M. L. Simpson, and L. S. Weinberger, *Cell* **173**, 1609 (2018).  
 [23] K. Exelby, E. Herrera-Delgado, L. G. Perez, R. Perez-Carrasco, A. Sagner, V. Metzis, P. Sollich, and J. Briscoe, *Development* **148**, dev197566 (2021).  
 [24] M. Lagha, J. P. Bothma, and M. Levine, *Trends Genet.* **28**, 409 (2012).  
 [25] G. Chalancon, C. N. Ravarani, S. Balaji, A. Martinez-Arias, L. Aravind, R. Jothi, and M. M. Babu, *Trends Genet.* **28**, 221 (2012).  
 [26] R. Perez-Carrasco, P. Guerrero, J. Briscoe, and K. M. Page, *PLoS Comput. Biol.* **12**, e1005154 (2016).  
 [27] B. Hu, W. Chen, W.-J. Rappel, and H. Levine, *Phys. Rev. Lett.* **105**, 048104 (2010).  
 [28] J. Cotterell and J. Sharpe, *Mol. Syst. Biol.* **6**, 425 (2010).  
 [29] A. Mugler, A. Levchenko, and I. Nemenman, *Proc. Natl. Acad. Sci. USA* **113**, E689 (2016).  
 [30] D. Ellison, A. Mugler, M. D. Brennan, S. H. Lee, R. J. Huebner, E. R. Shamir, L. A. Woo, J. Kim, P. Amar, I. Nemenman, *et al.*, *Proc. Natl. Acad. Sci. USA* **113**, E679 (2016).  
 [31] S. Artavanis-Tsakonas, M. D. Rand, and R. J. Lake, *Science* **284**, 770 (1999).  
 [32] D. Sprinzak, A. Lakhanpal, L. LeBon, L. A. Santat, M. E. Fontes, G. A. Anderson, J. Garcia-Ojalvo, and M. B. Elowitz, *Nature* **465**, 86 (2010).  
 [33] D. Sprinzak, A. Lakhanpal, L. LeBon, J. Garcia-Ojalvo, and M. B. Elowitz, *PLoS Comput. Biol.* **7**, e1002069 (2011).  
 [34] C. Kuyyamudi, S. N. Menon, and S. Sinha, *Phys. Biol.* (2021), 10.1088/1478-3975/ac31a3.  
 [35] R. Kopan and M. X. G. Ilagan, *Cell* **137**, 216 (2009).  
 [36] T. Erdmann, M. Howard, and P. R. Ten Wolde, *Phys. Rev. Lett.* **103**, 258101 (2009).  
 [37] A. D. Lander, *Cell* **144**, 955 (2011).  
 [38] H. L. Ashe and J. Briscoe, *Development* **133**, 385 (2006).  
 [39] J. C. Smith, *Curr. Opin. Cell Biol.* **7**, 856 (1995).

- [40] Y. Saka and J. C. Smith, *BMC Dev. Biol.* **7**, 1 (2007).
- [41] O. Barad, D. Rosin, E. Hornstein, and N. Barkai, *Sci. Signal.* **3**, ra51 (2010).
- [42] N. G. Van Kampen, *Stochastic Processes in Physics and Chemistry*, Vol. 1 (Elsevier, 1992).
- [43] D. J. Higham, *SIAM Rev.* **43**, 525 (2001).
- [44] J. H. Kong, L. Yang, E. Dessaud, K. Chuang, D. M. Moore, R. Rohatgi, J. Briscoe, and B. G. Novitch, *Dev. Cell* **33**, 373 (2015).
- [45] C. Kuyyamudi, S. N. Menon, and S. Sinha, *Phys. Rev. E* **103**, 062409 (2021).
- [46] B. Fuß and M. Hoch, *Curr. Biol.* **12**, 171 (2002).
- [47] M. L. Basch, R. M. Brown II, H.-I. Jen, F. Semerci, F. Depreux, R. K. Edlund, H. Zhang, C. R. Norton, T. Gridley, S. E. Cole, *et al.*, *eLife* **5**, e19921 (2016).

## SUPPLEMENTARY INFORMATION

### Precision of morphogen-driven tissue patterning during development is enhanced through contact-mediated cellular interactions

Chandrashekar Kuyyamudi, Shakti N. Menon and Sitabhra Sinha

#### LIST OF SUPPLEMENTARY FIGURES

1. Fig S1: Precision of cell fate determination resulting from interaction between stochastic gene expression dynamics and contact-mediated signaling measured in terms of steepness of spatial profile for expression of gene  $A$ .
2. Fig S2: Precision of cell fate determination resulting from interaction between stochastic gene expression dynamics and contact-mediated signaling measured in terms of steepness of spatial profile for expression of gene  $B$ .
3. Fig S3: The location  $l_B$  of the fate boundary in a linear array of cells resulting from different types of interaction between stochastic gene expression dynamics and contact-mediated signaling, in the presence of a morphogen gradient.



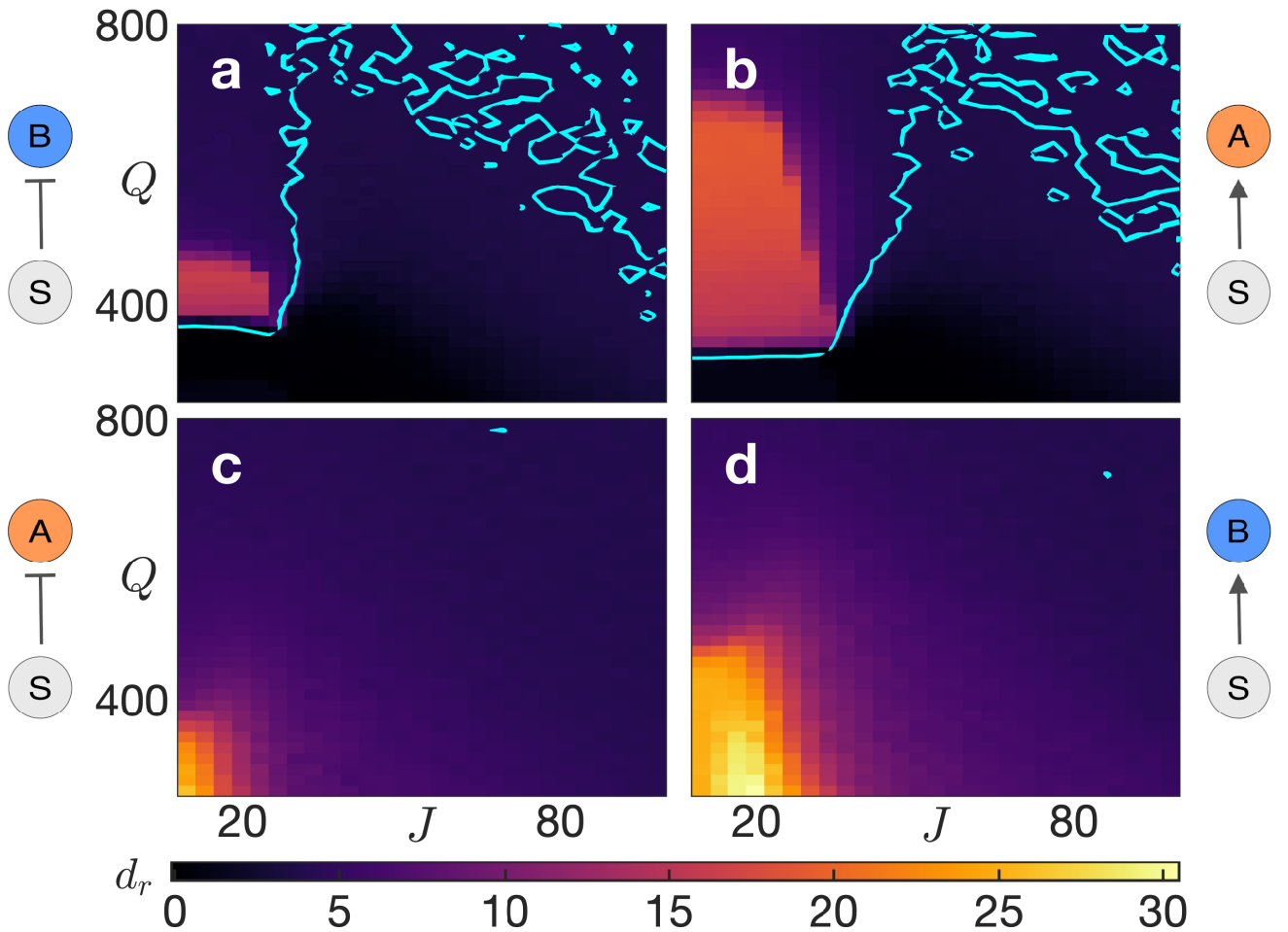


FIG. S1. **Precision of cell fate determination resulting from interaction between stochastic gene expression dynamics and contact-mediated signaling measured in terms of steepness of spatial profile for expression of gene  $A$ .** For each of the four types of interaction between the Notch downstream signal  $S$  and the patterning genes  $A, B$  (represented by the motifs shown beside each panel), the precision of the spatial pattern formed by cells adopting distinct fates  $A, B$  in a 1D domain comprising  $N(= 50)$  cells subject to a morphogen gradient is characterized by the slope of the growth in steady state expression levels of  $A$  across the cell array [the corresponding curve is shown in Fig. 1 (c) in the main text for the case when interactions are absent between cells]. This is measured by the rise distance, viz., the width (measured in terms of number of cells) over which  $A$  change from 10% to 80% of its maximum expression value for the type of interaction being considered. The mean rise distance ( $d_r$ ) across 300 stochastic realizations is shown for each choice of the pair of parameters quantifying the strength of intercellular coupling, viz.,  $J$  representing critical value of patterning gene expression segregating low/high receptor production and  $Q$  representing critical signal intensity that distinguishes between weak and strong regulation of patterning gene expression. The continuous curves in each panel are contours indicating the variance in  $d_r$  in the absence of intercellular interactions ( $\simeq 3.78$ ). Note that, for coupling types in which  $S$  upregulate  $A$  either directly (b), or indirectly via suppression of its inhibitor  $B$  (a), intercellular interactions are able to markedly increase the steepness of the spatial profile of gene expression, resulting in a sharply defined fate boundary, over a wider range of coupling strengths  $J$  and  $Q$ . In contrast, the resolution achieved with coupling types in which  $S$  upregulates  $B$  either directly (d), or indirectly via suppression of its inhibitor  $A$  (c), is almost always lower than even the uncoupled case.

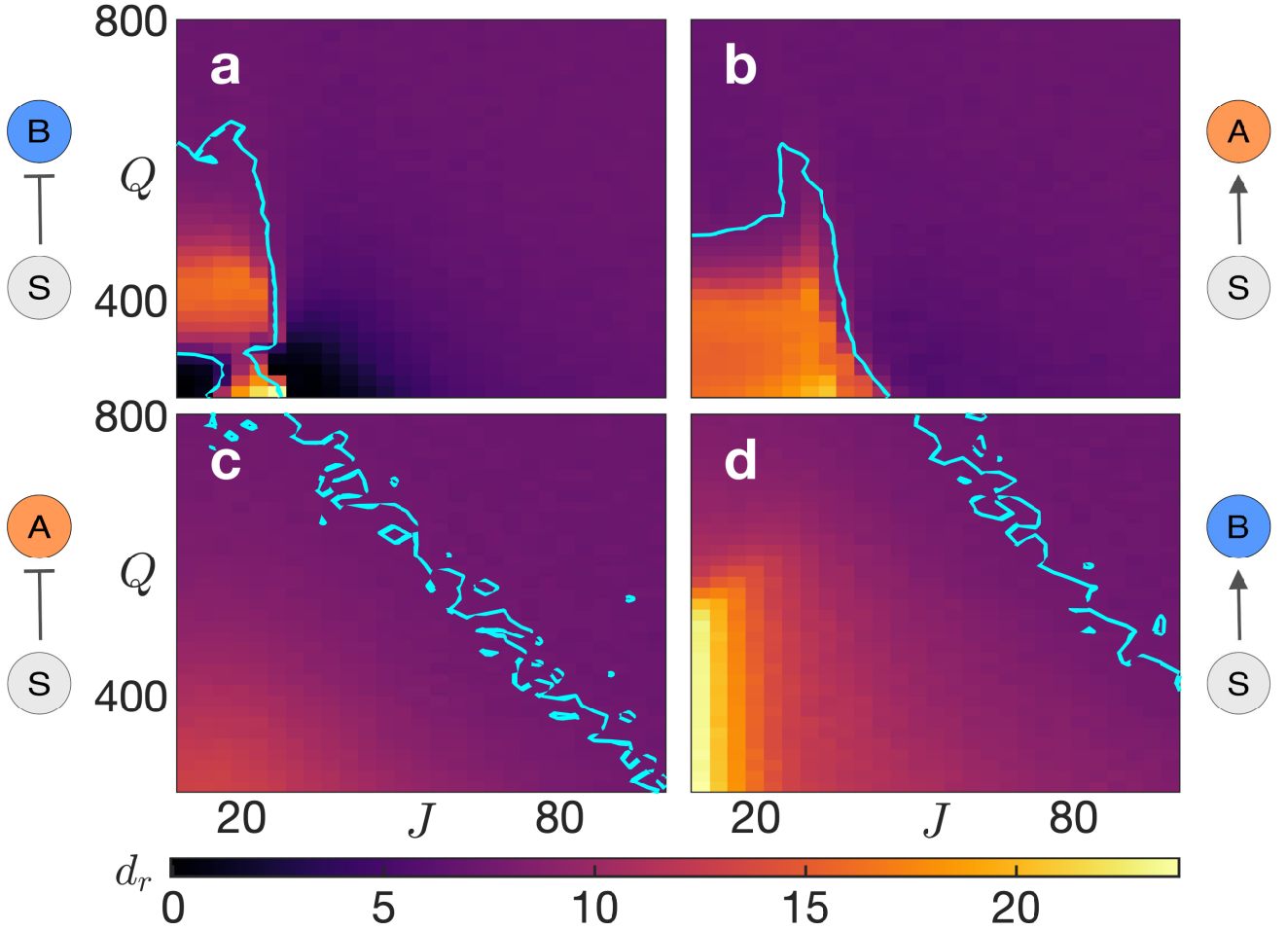


FIG. S2. **Precision of cell fate determination resulting from interaction between stochastic gene expression dynamics and contact-mediated signaling measured in terms of steepness of spatial profile for expression of gene  $B$ .** For each of the four types of interaction between the Notch downstream signal  $S$  and the patterning genes  $A, B$  (represented by the motifs shown beside each panel), the precision of the spatial pattern formed by cells adopting distinct fates  $A, B$  in a 1D domain comprising  $N(= 50)$  cells subject to a morphogen gradient is characterized by the slope of the decline in steady state expression levels of  $B$  across the cell array [the corresponding curve is shown in Fig. 1 (c) in the main text for the case when interactions are absent between cells]. This is measured by the rise distance, viz., the width (measured in terms of number of cells) over which  $B$  change from 80% to 10% of its maximum expression value for the type of interaction being considered. The mean rise distance ( $d_r$ ) across 300 stochastic realizations is shown for each choice of the pair of parameters quantifying the strength of intercellular coupling, viz.,  $J$  representing critical value of patterning gene expression segregating low/high receptor production and  $Q$  representing critical signal intensity that distinguishes between weak and strong regulation of patterning gene expression. The continuous curves in each panel are contours indicating the variance in  $d_r$  in the absence of intercellular interactions ( $\simeq 7.47$ ). Note that, for coupling types in which  $S$  upregulate  $A$  either directly (b), or indirectly via suppression of its inhibitor  $B$  (a), intercellular interactions are able to markedly increase the steepness of the spatial profile of gene expression, resulting in a sharply defined fate boundary, over a wider range of coupling strengths  $J$  and  $Q$ . The region of  $(J, Q)$  parameter space over which a higher resolution than the uncoupled case can be achieved is much reduced for the coupling types in which  $S$  upregulates  $B$  either directly (d), or indirectly via suppression of its inhibitor  $A$  (c).

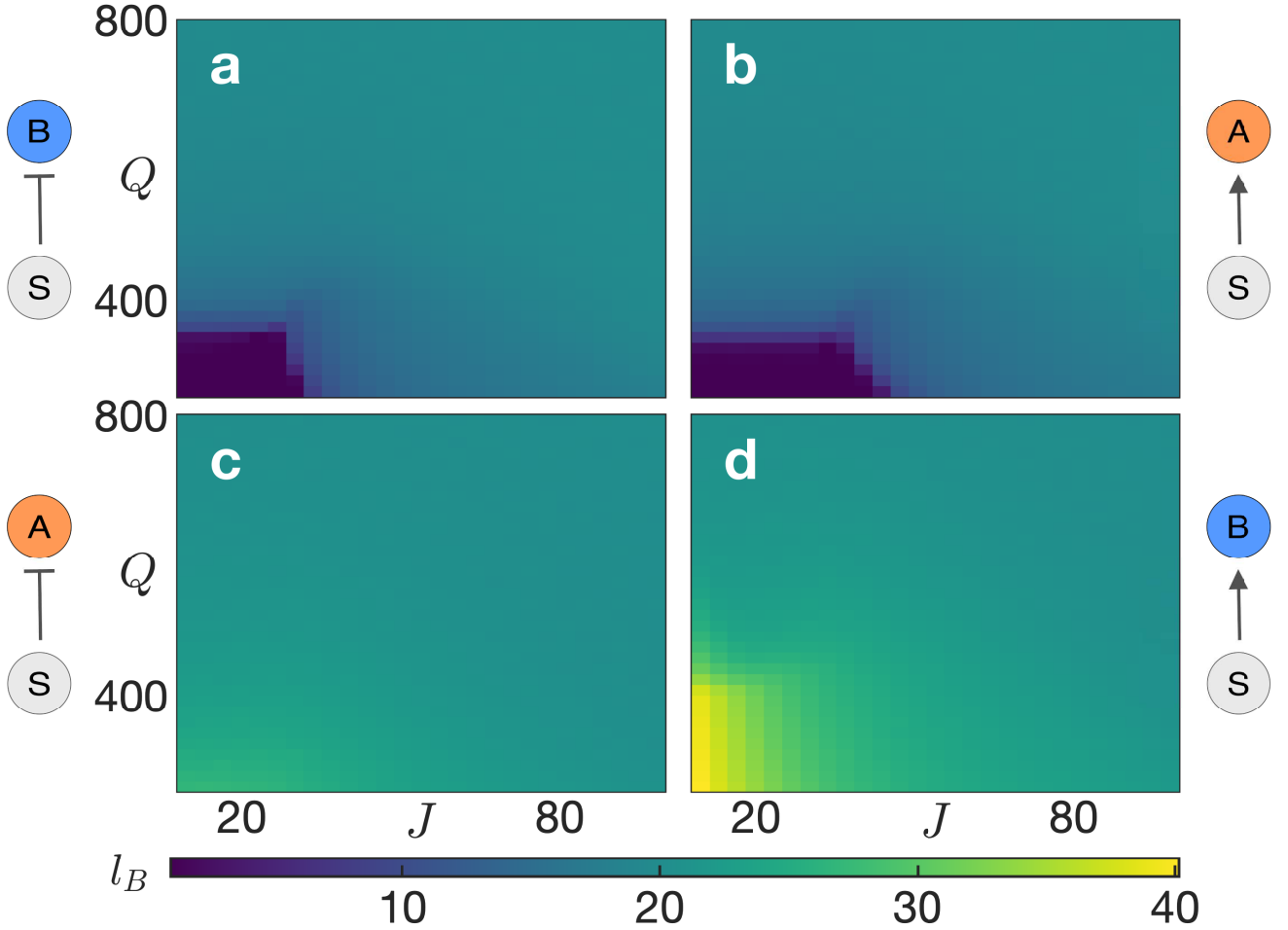


FIG. S3. The location  $l_B$  of the fate boundary in a linear array of cells resulting from different types of interaction between stochastic gene expression dynamics and contact-mediated signaling, in the presence of a morphogen gradient. For each of the four types of interaction between the Notch downstream signal  $S$  and the patterning genes  $A, B$  (represented by the motifs shown beside each panel), the spatial pattern formed by cells adopting distinct fates  $A, B$  in a 1D domain comprising  $N (= 50)$  cells subject to a morphogen gradient is characterized by the location  $l_B$  of the boundary [ $\sim 20$ , in absence of any interactions between the cells, see Fig. 1 (c) in main text] demarcating the segments expressing the two fates. The mean position of the boundary across 300 stochastic realizations is shown for each choice of the pair of parameters quantifying the strength of intercellular coupling, viz.,  $J$  representing critical value of patterning gene expression segregating low/high receptor production and  $Q$  representing critical signal intensity that distinguishes between weak and strong regulation of patterning gene expression. Note that, for coupling types in which  $S$  upregulate  $A$  either directly (b), or indirectly via suppression of its inhibitor  $B$  (a), intercellular interactions result in the fate boundary moves towards the morphogen source (in comparison to the uncoupled case). In contrast, the fate boundary moves further away from the morphogen source for coupling types in which  $S$  upregulates  $B$  either directly (d), or indirectly via suppression of its inhibitor  $A$  (c).